

Magnetic Domains and Stripes in a Spin-Fermion Model for Cuprates

Charles Buhler, Seiji Yunoki, and Adriana Moreo

Department of Physics, National High Magnetic Field Lab and MARTECH, Florida State University, Tallahassee, Florida 32306
(Received 26 August 1999)

Monte Carlo simulations applied to a model of interacting fermions and classical spins show the existence of antiferromagnetic spin domains and charge stripes upon hole doping. The stripes have a filling of approximately 1/2 hole per site, and they separate spin domains with a π phase shift among them. The observed stripes run either along the x or y axes. No particular boundary conditions or external fields are needed to stabilize these structures. When magnetic incommensurate peaks are observed at momentum $\pi(1, 1 - \delta)$, charge incommensurate peaks appear at $(0, 2\delta)$. The charge fluctuations responsible for the stripe formation also induce a pseudogap in the density of states.

PACS numbers: 74.20.Mn, 71.10.Fd, 74.25.Ha

In recent years neutron scattering experiments have established that magnetic incommensurability (MI) is a property common to most of the high- T_c cuprates [1]. In addition, there is mounting evidence supporting charge stripe formation in these compounds as well [2]. These nontrivial spin and charge arrangements may be crucial to understand the unusual transport and superconducting behavior of the cuprates. Phase separation between hole-rich and hole-poor regions in the CuO_2 planes, supplemented by long-range Coulomb interactions, has been proposed to explain the existence of stripes [3]. In addition, ground states with metallic stripes made out of d -wave hole pairs have been observed in the t - J model using open boundary conditions [4]. However, a more detailed theoretical understanding of these phenomena and resolution of current conflicting results have been extremely challenging especially since the t - J and Hubbard models used for the cuprates are considerably difficult to study.

As an alternative to this more traditional approach here a computational study of a simpler model involving interacting spins and fermions, the spin-fermion (SF) model, is presented. This model has been previously analyzed mostly using mean field approximations with the main goal of understanding d -wave superconductivity [5–8]. Here the focus is instead shifted toward its magnetic and charge properties, which have not been explored before using unbiased techniques. The SF model is constructed as an interacting system of electrons and spins, crudely mimicking phenomenologically the coexistence of charge and spin degrees of freedom in the cuprates [5–8]. Its Hamiltonian is given by

$$H = -t \sum_{\langle ij \rangle \alpha} (c_{i\alpha}^\dagger c_{j\alpha} + \text{H.c.}) + J \sum_{\mathbf{i}} \mathbf{s}_{\mathbf{i}} \cdot \mathbf{S}_{\mathbf{i}} + J' \sum_{\langle ij \rangle} \mathbf{S}_{\mathbf{i}} \cdot \mathbf{S}_{\mathbf{j}}, \quad (1)$$

where $c_{i\alpha}^\dagger$ creates an electron at site $\mathbf{i} = (i_x, i_y)$ with spin projection α , $\mathbf{s}_{\mathbf{i}} = \sum_{\alpha\beta} c_{i\alpha}^\dagger \boldsymbol{\sigma}_{\alpha\beta} c_{i\beta}$ is the spin of the mobile electron, the Pauli matrices are denoted by $\boldsymbol{\sigma}$, $\mathbf{S}_{\mathbf{i}}$ is the localized spin at site \mathbf{i} , $\langle ij \rangle$ denotes nearest-neighbor

(NN) lattice sites, t is the NN-hopping amplitude for the electrons, $J > 0$ is an antiferromagnetic (AF) coupling between the spins of the mobile and localized degrees of freedom (DOF), and $J' > 0$ is a direct AF coupling between the localized spins. The density $\langle n \rangle = 1 - x$ of itinerant electrons is controlled by a chemical potential μ . Hereafter $t = 1$ will be used as the unit of energy. From previous phenomenological analysis the coupling J is expected to be larger than t , while the Heisenberg coupling J' is expected to be smaller [6,7].

The value of the localized spin degrees of freedom requires a special discussion. When the model is derived directly from a three-band Hubbard model, the $\mathbf{S}_{\mathbf{i}}$ correspond to $S = 1/2$ Cu spins [6,7]. However, when they are considered as spin wave DOF, their value is not as clearly defined since the spin operators do not need to be $S = 1/2$ and they also can be nonlocal. Here, in order to simplify the numerical study it will be assumed that the spins are classical (with $|\mathbf{S}_{\mathbf{i}}| = 1$). The richness of the results reported below suggests that even in this classical approximation, crucial for the numerical analysis, the model produces nontrivial physics that resembles the high- T_c phenomenology. Then, although the classical spins cannot have spin damping, such a property seems *unnecessary* to produce $\langle n \rangle \approx 0.5$ stripes, behavior which appears regulated by the short-distance antiferromagnetic fluctuations present in both the classical and quantum models. Classical spins replacing quantum localized spins are also widely used in the context of manganite models where extensive work has shown that both cases lead to quite similar phase diagrams even for $S = 1/2$ [9].

The classical spin approximation allows us to perform Monte Carlo (MC) simulations of model Eq. (1) without “sign problems,” reaching by this procedure temperatures as low as $T = 0.01$ at any density. The value of J will be fixed to 2, as suggested in Ref. [7] where comparisons with experimental results were performed. The coupling J' among the classical spins will be set to 0.05. This value was selected by monitoring the magnetic susceptibility and comparing its behavior to experimental results for the cuprates [10]. The present study has been performed

mostly on 8×8 lattices with periodic boundary conditions (PBC), but occasional runs were made also using open and antiperiodic BC, as well as different lattice sizes. Details of the numerical method have been described in Ref. [9].

To study the magnetic properties of the system we measured the spin-spin correlation functions among the classical spins defined as $\omega(\mathbf{r}) = \frac{1}{N} \sum_{\mathbf{i}} \langle \mathbf{S}_{\mathbf{i}} \cdot \mathbf{S}_{\mathbf{i}+\mathbf{r}} \rangle$ (where N is the number of sites) whose Fourier transform provides the spin structure factor $S(\mathbf{q})$. The momentum q_γ takes the values $2\pi n/L_\gamma$, with n running from 0 to $L_\gamma - 1$, and L_γ denoting the number of sites along the $\gamma = x$ or y directions. In our MC simulations long-range AF order has been observed at $\langle n \rangle = 1.0$ as expected. As the electron density is reduced from 1, the $S(\pi, \pi)$ intensity decreases. One of the main results observed here occurs at finite hole density where a remarkable MI appears at $\langle n \rangle \approx 0.8$ with the structure factor peak moving to $\pi((1 - \delta), 1) = (3\pi/4, \pi)$ and rotated points. This behavior is illustrated in Fig. 1a where $S(\mathbf{q})$ on 8×8 lattices at $T = 0.01$ is shown for different values of $\langle n \rangle$ along the paths indicated. Note that the spin correlations along the two paths of Fig. 1a are different because at low temperatures the symmetry under lattice $\pi/2$ rotations appears spontaneously broken. Similar ground-state properties but rotated by $\pi/2$ have been observed in independent runs with different initial conditions for the classical spins [11] indicating that there are two energy minima separated by a large barrier. At $T = 0.05$ (Fig. 1b) and higher temperatures the rotational symmetry is restored, but the intensity of the incommensurate (IC) peaks is considerably reduced (e.g., at $\langle n \rangle = 0.75$ the $T = 0.01$ IC peaks are 4 times higher than at $T = 0.05$). To the extent that the SF and the

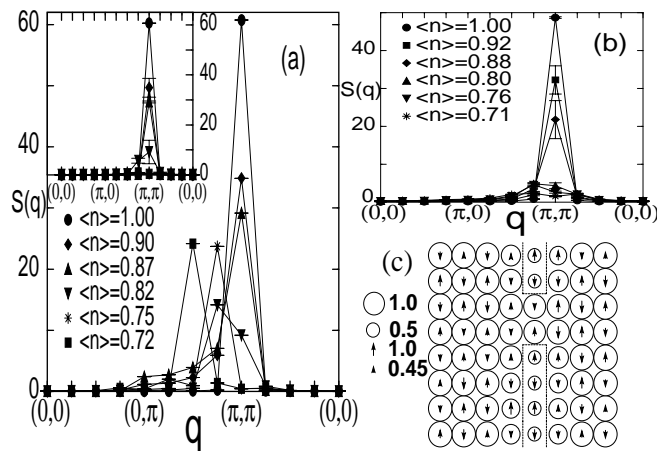


FIG. 1. (a) Structure factor $S(\mathbf{q})$ for the localized spins versus momentum for $J = 2$, $J' = 0.05$, and $T = 0.01$ on an 8×8 lattice and several densities along $(0,0)-(0,\pi)-(\pi,\pi)-(0,0)$ [inset: results along $(0,0)-(\pi,0)-(\pi,\pi)-(0,0)$]; (b) same as (a) but at $T = 0.05$; (c) spin and charge distribution for a typical MC snapshot at $\langle n \rangle = 0.9$ and the same parameters as in (a). The arrow lengths are proportional to the local spin $S_z(\mathbf{i})$ and the radius of the circles is proportional to the local density $n(\mathbf{i})$, according to the scale shown. PBC are used.

Hubbard models describe similar physics, this explains the low intensity of the IC peaks found in the $T = 0.2$ Hubbard model simulations [12].

Experimentally it was observed that $\delta \approx 0.25$ corresponds to the saturation value reached at hole density $x \approx 0.12$, which persists up to $x \approx 0.25$ [13]. Because of the finite size of the lattices studied here, MI for values of δ smaller than 0.25 cannot be detected, preventing us from comparing directly with the low-doping experimental results. However, we have analyzed typical spin configurations (snapshots) emerging from our MC simulations close to $\langle n \rangle = 1.0$, and we observed the existence of large AF spin domains in most of them, an example of which is shown in Fig. 1c for $\langle n \rangle = 0.9$. The existence of these domains clearly suggests that tendencies towards MI appear in the system at $x \leq 0.20$ as well.

The origin of the short-range IC magnetic order in the cuprates is still not clear. Magnetic order (MO) due to charge order (CO) has been proposed as a possible explanation. To explore the possibility of CO in model Eq. (1), we studied $N(\mathbf{q})$ defined as the Fourier transform of the charge correlations $n(\mathbf{r}) = \frac{1}{N} \sum_{\mathbf{i}} \langle (n_{\mathbf{i}} - \langle n \rangle)(n_{\mathbf{i}+\mathbf{r}} - \langle n \rangle) \rangle$, where $n_{\mathbf{i}}$ is the number operator at site \mathbf{i} for the itinerant fermions. In the AF phase at $\langle n \rangle = 1.0$, $N(\mathbf{q})$ was observed to present a broad peak at $\mathbf{q} = (\pi, \pi)$ due to negative charge correlations (charge repulsion) at very short distances, in agreement with previous calculations [14]. As the system is hole doped the behavior of $N(\mathbf{q})$ becomes more temperature dependent. At $T = 0.05$ the peak in $N(\mathbf{q})$ remains at (π, π) , but at $T = 0.01$ a sharp peak appears at small momenta for $0.7 < \langle n \rangle < 0.9$ (Figs. 2a and 2b) indicating the existence of extended charge structures. If charge and MI were related, stripe studies [2,3] predict that the peak in $N(\mathbf{q})$ has to appear at $(2\delta, 0)$ and symmetrical points. Then, incommensurability associated with $\delta = 0.125$, which cannot be explicitly detected in $S(\mathbf{q})$ due to the

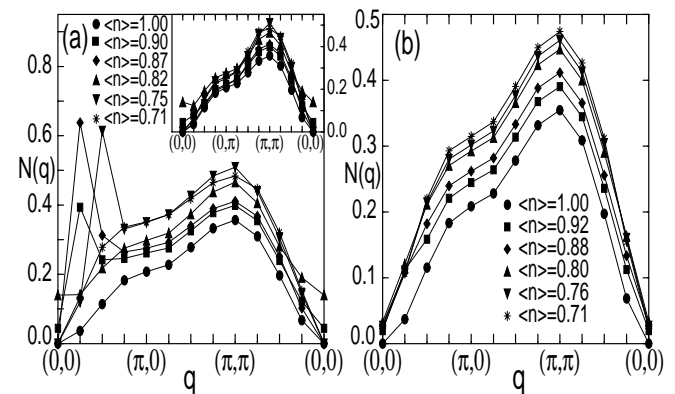


FIG. 2. (a) Structure factor $N(\mathbf{q})$ for the electrons versus momentum for $J = 2$, $J' = 0.05$, and $T = 0.01$ on an 8×8 lattice at several densities along the path $(0,0)-(\pi,0)-(\pi,\pi)-(0,0)$ [inset: same as main figure but along $(0,0)-(0,\pi)-(\pi,\pi)-(0,0)$]; (b) same as (a) but at $T = 0.05$. PBC are used.

size of our clusters, can nevertheless be observed in the charge channel. Indeed, in Fig. 2a the peak in $N(\mathbf{q})$ for density 0.87 is located at $\mathbf{q} = (\pi/4, 0)$ compatible with $\delta \approx 0.125$. At low temperature the peak can be observed along the x direction but not along y (see inset of Fig. 2a) indicating that in the MC runs described here the charge domains are along the y direction, causing the spontaneous breaking of rotational symmetry described before. This clearly can be seen in the charge distribution MC snapshot at $\langle n \rangle \approx 0.85$ shown in Fig. 3a. Note that the holes are located along the magnetic domain boundaries. The presence of stripes was explicitly verified also using 12×12 clusters [15]. The result is in excellent agreement with experiments [16] on Nd-doped $\text{La}_{2-x}\text{Sr}_x\text{CuO}_4$ (LSCO) where vertical stripes are observed at the Sr concentration $x \approx 1/8$.

In some stripe scenarios [17] CO is expected to occur at higher temperature than MO. However, in model Eq. (1) both CO and MO appear to occur at similar temperatures. Consider, for example, in Fig. 3b a typical MC snapshot at $\langle n \rangle = 0.75$ and $T = 0.01$. The holes are here aligned along *two* vertical columns. $S(\mathbf{q})$ and $N(\mathbf{q})$ for this particular snapshot are very similar to the averages shown in Figs. 1a and 2a, clearly indicating IC behavior in spin and charge. As the temperature is raised to $T = 0.05$, stripes are no longer observed (Fig. 3c) but there are still hole-poor magnetic domains which produce the (small) IC peak shown in Fig. 1b at this density. An equally weak feature appears in $N(\mathbf{q})$ but it is more difficult to distinguish because the background rises with increasing momentum,

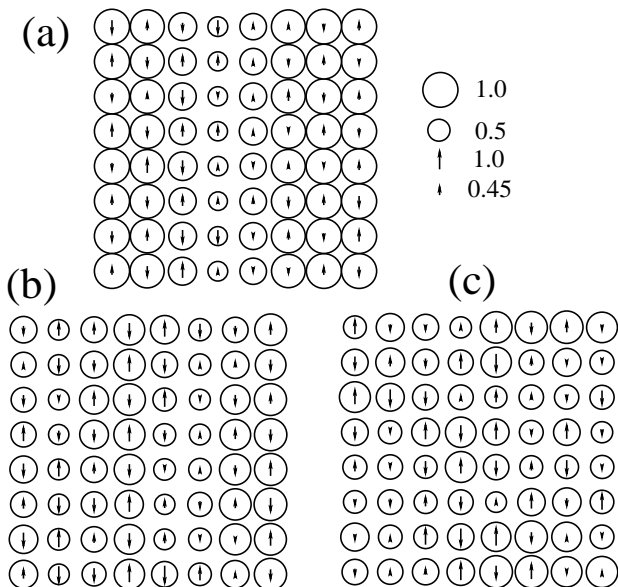


FIG. 3. (a) Spin and charge distribution for a MC snapshot on an 8×8 cluster for $J = 2$, $J' = 0.05$, $T = 0.01$, and at $\langle n \rangle \approx 0.85$; (b) spin and charge distribution for a snapshot at $\langle n \rangle = 0.75$ and the same parameters as in (a). The notation is as in Fig. 1c; (c) same as (b) but for $T = 0.05$. PBC are used. Only the z component of the spin is shown because it is the most representative in this case.

rather than being flat (Fig. 2b). This may be the reason why the MI is easier to detect than charge inhomogeneities in models such as Hubbard or t - J , where low temperatures are difficult to reach [12].

Our results are in qualitative agreement with the conclusions of Ref. [4,18] where it was argued that stripes can be stabilized at realistic values of J/t in the t - J model without the use of long-range Coulomb interactions. Moreover, in the SF model here we showed that charge stripes can appear spontaneously even with PBC, which are not practical in density matrix renormalization group calculations [18]. The SF model provides a clean and easy way to study toy model for the analysis of stripe formation in correlated electrons. The origin of the stripes in our study can be understood in part by analyzing the behavior of $\langle n \rangle$ vs μ shown in Fig. 4a, where it is observed that the density changes rapidly between 0.5 and 1. At $\langle n \rangle \approx 0.5$ there is a plateau indicating that this density is particularly stable. For $0.5 \leq \langle n \rangle \leq 1$ substantial charge fluctuations are to be expected due to the large value of $d\langle n \rangle/d\mu$, involving regions with density close to 1 (spin domains) and to 0.5 (hole stripes) which correspond to the two highly stable densities that appear in the system. In fact, calculating the charge density along the stripes we found that $0.5 \leq \langle n \rangle_{\text{stripe}} \leq 0.65$, which seems to indicate the existence of approximately one hole every two Cu ions. These stripes seem metallic according to their charge correlations which resemble results for metallic chains. The charge density on the hole-poor regions, on the other hand, has a value very close to 0.9. These densities inside and

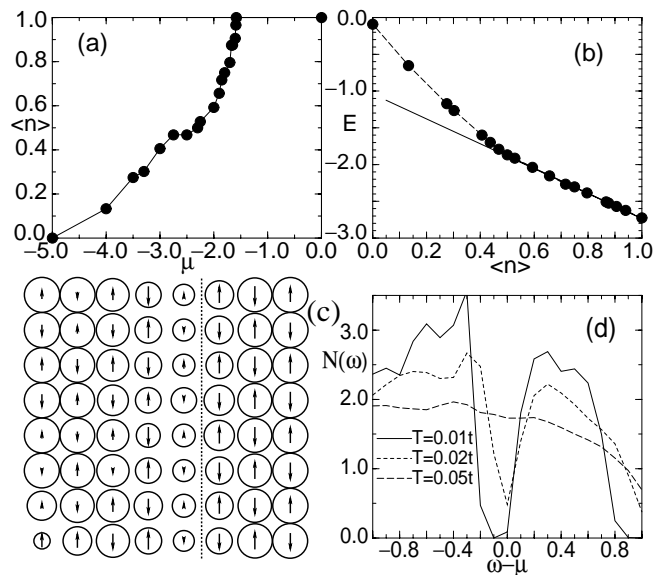


FIG. 4. (a) Density $\langle n \rangle$ vs μ for $J = 2$, $J' = 0.05$, and $T = 0.01$ on an 8×8 lattice with PBC; (b) energy versus density for the same parameters as in (a); (c) spin and charge distribution for a MC snapshot at $\langle n \rangle \approx 0.85$ and the same parameters as in (a) using OBC. The notation is as in Fig. 3; (d) density of states as a function of $\omega - \mu$ at $\langle n \rangle = 0.75$ for different temperatures. The remaining parameters are as in (a).

outside the stripe are in excellent agreement with experiments [2]. Then, the model studied here improves on early Hartree-Fock calculations that predicted a stripe density close to zero [19].

It is important to note that the SF model does not phase separate in spite of its large compressibility. Using different lattice sizes and BC we have verified that there is no discontinuity in $\langle n \rangle$ vs μ , while the energy presents a nearly straight line behavior in the density range between 0.5 and 1.0 (Fig. 4b).

As remarked before, stripe configurations were observed with several BC including periodic. One subtlety encountered in the latter is that for densities where a single stripe is stabilized the PBC prevented the occurrence of a π shift in the spin domains because it would induce spin frustration (Fig. 3a). However, if PBC are replaced by open BC (OBC) the stripe still appears and in this case a π shift is observed (Fig. 4c). When the number of stripes is even, as in Fig. 3b, the π shift is spontaneously obtained independently of the BC. This result is also in excellent agreement with experiments [16].

Our simulations can produce dynamical information directly in real frequency without the need of carrying out (uncontrolled) analytic extrapolations from the imaginary axis. This is particularly important to compare theoretical predictions with the results of recent photoemission experiments on optimally doped LSCO which showed the development of a pseudogap at μ as the temperature decreases [20]. In Fig. 4d we present the density of states (DOS) for $\langle n \rangle = 0.75$ at $T = 0.05, 0.02,$ and 0.01 . A pseudogap at $\omega = \mu$ develops for decreasing temperatures. This is a consequence of the strong density fluctuations discussed above, and it is similar to the phenomenon recently observed in the context of manganites where a pseudogap develops due to the coexistence of hole-rich and hole-poor domains [21].

To summarize, a model of interacting fermions and classical spins has been studied using MC techniques without *a priori* assumptions on their properties. Magnetic and charge incommensurability has been observed upon hole doping. The incommensurability is due to the formation of AF domains separated by stripes of holes. A π shift is observed between the domains, the stripes have some metallic characteristics, and they are partially filled with an electronic density of about 0.5. Charge and MI appear correlated, and stripelike configurations are obtained independently of the BC used and without the long-range Coulomb repulsion. The effect arises from the strong charge fluctuations between densities 0.5 and 1.0, which in addition produces a clear pseudogap in the DOS. Phase separation has not been observed in this study. It is interesting to

notice that early studies of related models also with classical spin backgrounds predicted incommensurability due to spiral phases [8,22] and diagonal stripes [23], but the complex behavior of model Eq. (1) reported here was not anticipated in previous analysis. This suggests that the SF model can be as useful for qualitative theoretical studies of the cuprates as the Hubbard and t - J models, while computationally it is considerably simpler.

A.M. is supported by NSF under Grant No. DMR-9814350. Additional support is provided by the National High Magnetic Field Lab and MARTECH.

-
- [1] S-W. Cheong *et al.*, Phys. Rev. Lett. **67**, 1791 (1991); P. Dai *et al.*, Phys. Rev. Lett. **80**, 1738 (1998); H. A. Mook *et al.*, Nature (London) **395**, 580 (1998).
 - [2] J. M. Tranquada *et al.*, Phys. Rev. Lett. **78**, 338 (1997).
 - [3] V. J. Emery *et al.*, Physica (Amsterdam) **209C**, 597 (1993); **235C**, 189 (1994), and references therein.
 - [4] S. R. White *et al.*, Phys. Rev. Lett. **80**, 1272 (1998); **81**, 3227 (1998).
 - [5] P. Monthoux *et al.*, Phys. Rev. B **47**, 6069 (1993); A. Chubukov, Phys. Rev. B **52**, R3840 (1995).
 - [6] J. R. Schrieffer, J. Low Temp. Phys. **99**, 397 (1995); B. L. Altshuler *et al.*, Phys. Rev. B **52**, 5563 (1995).
 - [7] C.-X. Chen *et al.*, Phys. Rev. B **43**, 3771 (1991).
 - [8] S. Klee *et al.*, Nucl. Phys. **B473**, 539 (1996).
 - [9] E. Dagotto *et al.*, Phys. Rev. B **58**, 6414 (1998).
 - [10] We also tested our model by calculating the one-particle spectral function $A(\mathbf{q}, \omega)$ at $\langle n \rangle = 1$. Excellent agreement with results for the t - J model [A. Moreo *et al.*, Phys. Rev. B **51**, 12045 (1995); S. Haas *et al.*, Phys. Rev. Lett. **74**, 4281 (1995)] was found, including the presence of shadow bands.
 - [11] The initial conditions when not otherwise specified are random disordered spin configurations.
 - [12] A. Moreo *et al.*, Phys. Rev. B **41**, 2313 (1990); D. Duffy and A. Moreo, Phys. Rev. B **52**, 15607 (1995).
 - [13] K. Yamada *et al.*, Phys. Rev. B **57**, 6165 (1998).
 - [14] Y. C. Chen *et al.*, Phys. Rev. B **50**, 655 (1994).
 - [15] Notice that the use of classical spins does not necessarily promote CO. For example, in similar models for manganites, CO is not observed [9].
 - [16] J. M. Tranquada *et al.*, Nature (London) **375**, 561 (1995).
 - [17] O. Zachar *et al.*, Phys. Rev. B **57**, 1422 (1998).
 - [18] G. Martins *et al.*, Phys. Rev. B **60**, R3716 (1999); S. White and D. Scalapino, e-print cond-mat/9907375.
 - [19] D. Poilblanc *et al.*, Phys. Rev. B **39**, 9749 (1989); J. Zaanen *et al.*, Phys. Rev. B **40**, 7391 (1989).
 - [20] T. Sato *et al.*, Phys. Rev. Lett. (to be published).
 - [21] A. Moreo *et al.*, Phys. Rev. Lett. **83**, 2773 (1999).
 - [22] B. Shraiman *et al.*, Phys. Rev. Lett. **62**, 1564 (1989).
 - [23] T. Dombre, J. Phys. (Paris) **51**, 847 (1990).